Combining Bone Collagen Matrix with HUC-MSCs for Application to Alveolar Process Cleft in a Rabbit Model

Xue-Cheng Sun (375953879@qq.com)
Reproductive and Genetic Center of National Research Institute for Family Planning
https://orcid.org/0000-0002-1689-2627

Hu Wang
Reproductive and Genetic Center of National Research Institute for Family Planning

Dan Zhang
Reproductive and Genetic Center of National Research Institute for Family Planning

Jian-Hui Li
Reproductive and Genetic Center of National Research Institute for Family Planning

Li-Qiang Yin
Yantai Zhenghai Bio-Tech Co., Ltd.

Yu-Fang Yan
Yantai Zhenghai Bio-Tech Co,. Ltd.

Xu Ma
Reproductive and Genetic Center of National Research Institute for Family Planning

Hong-Fei Xia
Reproductive and Genetic Center of National Research Institute for Family Planning

Research Article

Keywords: Alveolar process cleft, Bone collagen matrix, Japanese white rabbits (JWRs), Human umbilical cord mesenchymal stem cells (hUC-MSCs), Micro-focus computerized tomography (micro-CT)

Posted Date: July 2nd, 2021

DOI: https://doi.org/10.21203/rs.3.rs-335429/v2

Version of Record: A version of this preprint was published at Stem Cell Reviews and Reports on August 22nd, 2021. See the published version at https://doi.org/10.1007/s12015-021-10221-y.

Abstract

Background: Most materials used clinically for filling severe bone defects either cannot induce bone regeneration or exhibit low bone conversion, therefore, their therapeutic effects are limited. Human umbilical cord mesenchymal stem cells (hUC-MSCs) exhibit good osteoinduction. However, the mechanism by which combining a heterogeneous bone collagen matrix with hUC-MSCs to repair the bone defects of alveolar process clefts remains unclear.

Methods: A rabbit alveolar process cleft model was established by removing the bone tissue from the left maxillary bone. 48 young Japanese white rabbits (JWRs) were divided into normal, control, material and MSCs groups. An equal volume of a bone collagen matrix alone or combined with hUC-MSCs was implanted in the defect. X-ray, micro-focus computed tomography (micro-CT), blood analysis, histochemical staining and TUNEL were used to detect the newly formed bone in the defect area at 3 and 6 months after the surgery.

Results: The bone formation rate obtained from the skull tissue in MSCs group was significantly higher than that in control group at 3 months (P<0.01) and 6 months (P<0.05) after the surgery. The apoptosis rate in the MSCs group was significantly higher at 3 months after the surgery (P<0.05) and lower at 6 months after the surgery (P<0.01) than those in the normal group.

Conclusions: Combining bone collagen matrix with hUC-MSCs promoted the new bone regeneration in the rabbit alveolar process cleft model through promoting osteoblasts formations and chondrocyte growth, and inducing type 1 collagen formation and BMP-2 generation.

Introduction

An alveolar process cleft is a common clinical diagnosis of alveolar bone defects caused by birth defects, trauma, or inflammation, which severely affects a patient's facial and oral functions. It also greatly hinders the patient's subsequent denture repair. The goal of alveolar bone reconstruction is to generate physiologically functioning bone and eventually restore facial morphology and occlusal function. Currently, autogenous bone transplantation remains the clinical gold standard and, commonly autogenous bone includes the skull [1], cancellous bone [2], ilium [3], etc. In addition, there are dozens of bone substitutes, such as allogeneic [4], alloplastic [5] and tissue-engineered [6], bones have been applied in clinical practice.

The ideal bone repair material must exhibit numerous properties. On the one hand, it should have a wide range of readily available sources, and exhibit high bio-compatibility and safety. On the other hand, it must also exhibit certain plasticity and bio-degradability. In addition, it must exhibit good bone conductivity and inductance. The collagen matrix used in this study was prepared by refining bovine cancellous bone through a series of de-cellularizaisation and degreasing processes. Its main components are hydroxyapatite and collagen. The material not only exhibited greatly reduced immunogenicity, but also maintained the natural bone structure. The material has a suitable pore size for facilitating the

growth of cells and blood vessels. Because the bone re-generation environment is complex, it is difficult to meet bone re-generation requirements using only a bone collagen matrix. Studies have shown that human umbilical cord mesenchymal stem cells (hUC-MSCs) play an important role in inducing bone regeneration [7–9]. HUC-MSCs have the advantages of wide availability, rapid proliferation and low immunogenicity [9]. Furthermore, because foetal umbilical cords are considered medical waste, hUC-MSCs have low ethical controversy. Therefore, in this study, hUC-MSCs were inoculated into a bone collagen matrix to induce bone regeneration and repair.

Developing a suitable animal model of an alveolar bone defect according to the clinical characteristics of oral bone grafting surgery is the basis and focus of studying alveolar bone repair and evaluating the osteogenic ability of bone grafting materials. Many researchers have used monkey [10], beagle [11–12], miniature pig [13–14], rabbit [15], rat [16] and other experimental animals to develop bone defect models in different parts of the animals' jaws. After the bone material was implanted, the ability to reconstruct the jawbone was assessed using pathology methods. Compared with other animals, rabbits have the advantages of a short growth cycle, easy feeding and low cost. Furthermore, because rabbits exhibit a moderate body size and gentle temperament, they are easier to handle than many other animals. Therefore, many researchers have also used rabbits as models of alveolar process clefts [17–19].

In this study, Japanese white rabbits (JWRs) were selected based on our previous research findings [20], and part of their left maxilla was surgically removed to prepare alveolar process cleft models. Because rabbits have more blood supply sources and stronger self-healing ability than humans, the bone defect should be the critical size defect (CSD) [15]. This model provides an important basis for evaluating the osteogenic capacity of the bone collagen matrix inoculated with hUC-MSCs.

Materials And Methods

Isolation and culture of hUC-MSCs

The hUC-MSCs were obtained by tissue mass culture. Briefly, the blood vessels of the human umbilical cord were removed, and then the cord was cut into approximately 1 mm^3 of tissue. Until tissue block was attached to the bottom of the cell culture dish, α-Minimal Essential Medium (α-MEM) culture medium containing 10% fetal bovine serum, 100 IU/mL penicillin, and 10 mg/mL streptomycin was added to the dishes and cultured in a carbon dioxide incubator. The cell growth was monitored, and the tissue was removed when the cells had radially covered the surface of the culture plate. The surface antigens of within 5 passages cells were detected using a human MSC assay kit (BD Biosciences Franklin Lakes, NJ, USA).

Preparation Of Implant Materials

The bone collagen matrix is a heterogeneous bone matrix prepared from bovine cancellous bone refined in a series of processes, thereby retaining its natural three-dimensional porous structure. The main

components of the bone collagen matrix are hydroxyapatite and collagen. The collagen membrane coverings the site after the bone collagen matrix was implanted. The collagen membrane was approximately 0.8 mm thick. Before use, the collagen membrane was cut into small pieces the same size as the defect area. The bone collagen matrix and collagen membrane were both provided by Zhenghai Bio-technology Co., Ltd (Yantai, China). The hUC-MSCs within five passages were harvested and suspended in phosphate buffer solution (PBS) at the concentration of 10^7 cells/ mL.

Groups And Treatment

In this study, 48 female JWRs (bodyweight: 2000 ± 300 g, about two-month-old) were used. The JWRs were purchased from Huafukang Bio-technology Co., Ltd (Beijing, China). All these animals were kept in the animal room at the National Research Institute for Family Planning. and were provided with clean water and fresh food. The indoor conditions were as follows: temperature (24 ± 1℃); air humidity (55% ±5%); noise (less than 60dB); lighting time (12 h). The room always was kept clean, dry and ventilated. The experimental design and implementation were approved by the local research and ethics committee.

In this study, JWRs were randomly assigned to each of four groups: normal, control, material, and MSCs. The rabbits were first anesthetised by an intravenous injection of serazine hydrochloride into the ear margin (concentration: 1–2 mg/kg) and then the left maxilla was located. The alveolar process cleft model was established by removing part of the jawbone equal to the volume of 1cm · 0.5 cm · 0.4 cm with a rongeur (Fig. 1).

The normal group was fed normally. In the control group, after part of the jawbone was removed, the collagen membrane was used to directly cover the injury, and the muscles and skin at the injured site were sutured. In the material group, part of the jawbone was removed, the same volume of the bone collagen matrix was implanted in the injury, and then the collagen membrane was used to directly cover the injury, and the muscles and skin of the injured site were sutured. In the MSCs group, bone collagen matrix (1cm · 0.5 cm · 0.4 cm) was inoculated with 10^7 cells/mL hUC-MSCs suspension and cultured in a carbon dioxide incubator for 0.5 h. After part of the jawbone was removed, combining bone collagen matrix with hUC-MSCs was implanted and then the collagen membrane was used to directly cover the injury, and the muscles and skin of the injured site were sutured. Conventional anti-inflammatory therapy (i.e. penicillin potassium: 4000 IU/kg/d) was then given to all the rabbits for 1 week to prevent postoperative infection. The rabbits were removed from each group at 3 and 6 months after the surgery. The rabbits were euthanised by intravenous injection of an overdose of serazine hydrochloride in the ear margin. The skull was removed, and partial skulls were placed in 4% NaOH and 95% ethanol respectively for 24h, and then taken out and placed in an oven to dry. Finally, the appearance of the skull tissue was photographed and marked. Partial fresh skull tissue was first fixed in 4% paraformaldehyde for 24h, de-calcified with 10% ethylenediaminetetraacetic acid (EDTA) for 1 month, and finally embedded in paraffin. The paraffin sections (6 μm) were prepared using a rotary microtome (Leica RM2245, Leica, GmbH,

Germany). For histology staining, the paraffin sections were first de-paraffinized in xylene and then re-hydrated in graded alcohol solutions to pure water.

X-ray Analysis

X-ray analysis was performed using a SOFTEX® M-60 X-ray machine (Kanagawa, Japan) operated at 80 kV and 125 mA on the tissue samples prepared from the surgical sites in each group at 3 and 6 months after the surgery at the Beijing Ornamental Animal Hospital. The exposure time was 40 millisecond (ms).

Serum Bone Gla Protein (Bgp) Analysis

Three rabbits were randomly selected from each group at 3 and 6 months after the surgery. Approximately 3.5mL of blood was collected by ear-vein sampling. Some of the blood was used for direct detection and the remainder for serum separation. The blood routine, liver function, renal function and serum BGP of the rabbits were all measured. The routine blood tests were performed using an LH 750 automated haematology analyser (Beckman Coulter, USA). The blood biochemistry test was performed using a DXC 800 automated biochemical analyser (Beckman Coulter, USA).

Bone Formation Rate Analysis

Three rabbit skull models were randomly made in each group at 3 and 6 months after surgery, respectively. The lateral view of the surgical side of the rabbit was obtained by photographing. Then, the actual bone defect area and the total bone defect area were measured by Image J, and the difference value between the two was the area of new osteogenesis. The percentage of osteogenic area to defect area is the bone formation rate.

Micro-focus Computed Tomography (Micro-ct) Analysis

Three rabbits were randomly selected from each group at 3 and 6 months after the surgery. A skull model was prepared. The general appearance of the skull was recorded laterally and vertically. The bone re-generation in the material transfer area in the material transfer area were evaluated using a micro CT system (SIEMENS Inveon™ Research Workplace 4.2, Beijing). The repair of the maxillary region in each group was observed stereoscopically. In order to analyse the the quality of the newly formed bone in the defect area, three 1 mm^3 areas were randomly selected from the centre of the cubic bone-defect area in each group to record the bone trabeculae and mineral density.

Hematoxylin And Eosin (He) Staining

HE staining was used to observe the tissue morphology. The nucleus and other areas were stained blue and red by the hematoxylin and eosin respectively. A TE2000-U inverted phase contrast microscope (Nikon, Tokyo, Japan) was used to observe the changes in the bone histomorphology.

Periodic Acid-schif (Pas) Staining

PAS staining was used to assess the glycogen concentration and was performed using a commercial kit (Senbeijia Biological Technology Co. Ltd, NanJing, Jiangsu, China) according to the manufacturer's instructions. Briefly, the sections were incubated in the dark first with periodic acid solution and then with the Schiff reagent for 5 and then 20 min at room temperature, respectively. The sections were then counterstained with Lillie-Mayer's hematoxylin and were observed using differential interference contrast (DIC) optics microscopy (DM IL LED, Leica GmbH, Germany). The cartilage structure can be dyed either deep purple or red.

Sirius red staining

Sirius red staining was used to detect different collagen fibers and was performed using a commercial kit (Senbeijia Biological Technology Co. Ltd, Nanjing, Jiangsu, China) according to the manufacturer's instructions. Briefly, the sections were incubated with sirius red for 1 h at room temperature and counter-stained with Lillie Mayer's hematoxylin. Sirius red can dye type 1 collagen bright orange. Image J software was used to calculate the relative percentage of the type 1 collagen stained area under different fields in each group.

Bone-specific alkaline phosphatase (ALP) assay

Bone-specific ALP is an osteoblasts phenotypic markers, which can directly reflect the activity or function of osteoblasts. ALP calcium-cobalt staining was used to detect the bone-specific ALP content by a commercial kit (KeyGEN BioTECH Co.Ltd, NanJing, Jiangsu, China) used according to the manufacturer's instructions. Briefly, the sections were incubated with ALP solution for 5 min and then with cobalt nitrate solution for 2 min at room temperature. The sections were then counter stained with eosin. The osteoblasts can be dyed black.

Immunohistochemical Staining For Bone Morphogenetic Protein 2 (Bmp-2)

After the sections were de-waxed, re-hydrated and subjected to heat-induced epitope retrieval, they were incubated with rabbit anti-BMP-2 polyclonal antibody (1:1000; Abcam, ab6285, Cambridge, UK), and then incubated with HRP-conjugated goat anti-rabbit IgG (1:5000; Jackson ImmunoResearch Laboratories, West Grove, Pennsylvania, USA). Normal rabbit serum was used as blocking solution. The sections were

developed with diaminobenzidine tetrahydrochloride (DAB) and counterstained with hematoxylin. Samples were viewed at Leica inverted microscope (Leica, Wetzlar, Germany). Three different sections were chosen for the same animal. There are at least three animals in each group. Three fields were randomly selected for each section, and the mean optical densities (MOD) of positive signals of BMP-2 were analyzed using Image J software. The percentage of MOD of BMP-2 signals were expressed as ratio of MOD of BMP-2 signals vs total signals.

Immunofluorescence For Ki67

The sections were incubated with mouse anti Ki-67 monoclonal anti-body (1:200; Abcam, ab15580, Cambridge, UK), and then incubated with fluorescein isothiocyanate (FITC)-conjugated goat anti-mouse IgG (1:300; Jackson ImmunoResearch Laboratories, West Grove, Pennsylvania, USA). Goat serum was used as blocking solution. Nuclei were stained with Hoechst 33258. Sections were viewed under a laser-scanning confocal microscope (ZEISS LSM 710 META, Oberkochen, Germany). Three different sections were chosen for the same animal. There are at least three animals in each group. The proliferative cells labeled by Ki67 were counted in three different optical fields selected in a random manner, and counted at least 100 cells for each section. The percentage of proliferative cells were expressed as ratio of Ki67-positive cells vs the total number of cells.

Detection of apoptosis assay by TdT-mediated dUTP nick-end Labelling (TUNEL)

TUNEL assays were prepared using an in-situ Cell Death Detection Kit, Fluorescein (Roche, Mannheim, Germany) according to the manufacturer's instructions. To correlate the TUNEL assay results with the nuclear morphology, the sections were counterstained with hematoxylin. The number of apoptotic cells was counted in 3 randomly selected optical fields (magnification ×400). The samples were by Leica inverted microscope (Leica, Wetzlar, Germany). At least 100 randomly selected cells in each sample were evaluated for apoptosis in the different optical fields (magnification ×400). The results were expressed as the ratio of TUNEL-positive cells to the total number of cells. Each sample was observed at least three times. The TUNEL analysis was performed 3 times for each animal, and the average value was used for the statistical analysis.

Statistical analysis

The results are presented as mean ± standard deviation (SD), and $P < 0.05$ is considered statistically significant. The data from the blood, HE staining, Sirius red staining, PAS staining, ALP staining immunohistochemical tests and TUNEL were statistically analyzed using one-way analysis of variance (ANOVA). The difference of the bone trabeculae and mineral density between injury side and normal side was analyzed using Student's *t*-test.

Results

HUC-MSCs express specific surface antigens

The hUC-MSCs used in this study were previously identified by our lab [21]. Before the experiment, the surface antigen of hUC-MSCs was identified again. The expression of positive markers for MSC such as CD73, CD105, CD90, and CD44 of the hUC-MSC were detected almost above 95%. The expression of negative markers for MSC such as CD34, CD11b, CD19, CD45, and HLA-DR were all below 5%. These facts are consistent with the characteristics of MSCs [22].

Morphometric Analysis Of Alveolar Process Tissues

The injury and normal sides in each group were compared by visual inspection. At 3 months after the surgery, little repair was found in the bone defect area of the material and control groups, while partial repair was found in the bone defect area of the MSCs group (Fig. 2A). At 6 months after the surgery, there was slightly repair in the bone defect area of the material and control groups. In MSCs group, the degree of bone repair in the bone defect site was close to the normal bone observed from the external appearance (Fig. 2B). The bone formation rate in MSCs group was significantly higher than that in control group at 3 months ($P < 0.01$) and 6 months ($P < 0.05$) after the surgery, respectively (Fig. 2C and D). Although bone collagen matrix alone did not significantly increase the bone defect area, it induced slight bone regeneration.

To evaluate the degree of bone repair in the alveolar process cleft, X-ray analysis was used for the preliminary analysis in which bone density was positively correlated with brightness (Fig. 3). Compared with the brightness (an indicator of bone density) of the normal group, those of the control, material, and MSC groups were the lowest, mid-range, and highest at 3 months after the surgery. At 6 months after the surgery, the brightness of the MSCs group remained higher than those of the other groups. Therefore, the osteogenic effect of combining the bone collagen matrix with the hUC-MSCs may be observably stronger than that obtained for only the bone collagen matrix.

To further analyze the absorption of the bone materials and the bone formation of the alveolar process cleft, micro-CT scans were conducted to detect the skull tissues from different perspectives at 3 (Fig. 4A) and 6 months (Fig. 4B) after the surgery. The injury and normal sides were compared in each group. The micro-CT scans were consistent with the visual inspection. Compared with the control and material groups, the MSCs groups had more visible new bone formation in the bone defect site at 3 months after surgery (Fig. 4A) and were close to normal bone morphology at 6 months after surgery (Fig. 4B). The percentage of the bone density and trabecular bone were then calculated for each group (Fig. 4C). At 3 months after the surgery (Fig. 4Ca), the percentage of the trabecular bone in the MSCs group (60.916 ± 2.072 %) was the highest, followed by the material group (52.647 ± 2.857 %) and the control group was 0. The results obtained at 6 months after the surgery were like those obtained at 3 months after the surgery (Fig. 4Cc; MSCs group: 73.338 ± 2.132 %, material group: 61.180 ± 4.241 %, control group: 0). The results showed that the percentage of bone density in the control group (0.466 ± 0.110 %) was the lowest and

that the material (53.013 ± 2.002 %) and MSCs groups (64.337 ± 2.011 %) were negligibly different 3 months after the surgery (Fig. 4Cb). The percentage of the bone density in the MSCs group (82.936 ± 2.112 %) was significantly higher than that in the other two groups (material group: 43.858 ± 0.522 %, control group: 1.29 ± 0.522 %) at 6 months after the surgery (Fig. 4Cd). Therefore, the osteogenic ability and the quality of the newly formed bone of combining the bone collagen matrix with the hUC-MSCs was higher than that of only the bone collagen matrix.

Microscopic structure of bone defect site detected by HE staining

HE staining showed that no significant bone repair was observed in the control group at both 3 and 6 months after the surgery (Fig. 5 Aa1 & Ae1). At 3 months after the surgery, a few bone fibers, some bone marrow and trabeculae, and numerous cavitation structures were observed in the damaged area in the material group (Fig. 5 Ac1). At 6 months after the surgery, trabecular bone, bone marrow, and cavitation structures were observed in a few of the bone repair areas in the material group (Fig. 5 Ag1). In the MSCs group, no cavitation was observed in the damaged area at 3 months after the surgery, and numerous bone trabeculae and fibrous tissues were observed (Fig. 5 Ad1). At 6 months after the surgery, the bone trabeculae in the damaged area of the MSCs group had connected to form bone tissue (Fig. 5 Ah1). These results indicate that the MSCs group shows better repair.

Measurement Of Serum Bone Gla Protein (Bgp)

BGP is a bone-specific-protein synthesized by osteoblasts and is incorporated into the bone matrix. The serum BGP results showed that the BGP concentrations in the control and material groups were approximately equal to and significantly enhanced in the MSCs groups at 3 months after the surgery ($P < 0.05$; Fig. 5B1). These results show that the osteogenic ability of combining the bone collagen matrix with the hUC-MSCs was higher than that of only the bone collagen matrix.

Effects of bone collagen matrix combined with hUC-MSCs on osteoblasts, collagen, and bone-formation-associated saccharides

ALP staining was used to detect the black-stained osteoblasts. The results showed that the normal maxillary bone exhibited a uniform matrix without any osteoblasts (Fig. 6 Aa & Ae). The ALP staining results obtained at 3 and 6 months after the surgery were then compared. The control group showed no obvious black areas (Fig. 6 Ab & Af). In the material group, although black appeared at the edge of the trabecular bone at 3 months after the surgery (Fig. 6 Ac), and no black area was observed at 6 months after the surgery (Fig. 6 Ag). In the MSCs group, black appeared at the edge of the trabecular bone at 3 months after the surgery (Fig. 6 Ad), and remained at 6 months after the surgery (Fig. 6 Ah). The percentages of ALP-stained signals at 3 and 6 months after the surgery in the material group were approximately equal to those in the normal group, while those in the MSC group were significantly higher than those in the other groups ($P < 0.01$; Fig. 6B1 & B2). The results show that combining the bone

collagen matrix with the hUC-MSCs can promote osteoblasts formations better than the bone collagen matrix alone.

Sirius red staining is used to analyze the collagen distribution and can dye type 1 collagen bright orange. The sirius red stain revealed the uniform distribution of type 1 collagen in the normal maxillary bone (Fig. 7 Aa & Ae). In the control group, only a very small amount of type 1 collagen was present (Fig. 7 Ab & Af). In the material group, a small amount of collagen type 1 was observed in the bone defect area after the implantation of only the bone collagen matrix (Fig. 7 Ac & Ag). However, after the implantation of the bone collagen matrix combined with the hUC-MSCs, a large amount of collagen type 1 was observed in the bone-defect area (Fig. 7 Ad & Ah). The statistical results showed that the collagen type 1 content in the MSCs group was approximately equal to that in the normal group (Fig. 7B & C). The type 1 collagen contents in the control and material groups were significantly lower than that in the normal group ($P < 0.01$). These results show that combining the bone collagen matrix with the hUC-MSCs could induce type 1 collagen formation more effectively than only the bone collagen matrix.

Saccharide is a constituent of cartilage-matrix constituent, and PAS staining was used to assay the saccharide content. The results showed that the normal maxillary bone exhibited a uniform matrix without any chondrocytes (Fig. 8 Aa & Ae). The PAS staining results obtained at 3 and 6 months after the surgery were then compared. The control group did not exhibit any obvious red or fuchsia areas at either 3 or 6 months after the surgery (Fig. 8 Ab &A f). At 3 months after the surgery, the trabecular bone border in the material group appeared red or fuchsia (Fig. 8 Ac) and was reduced at 6 months after the surgery (Fig. 8 Ag). At 3 months after the surgery, the trabecular bone of the MSCs group showed large fuchsia areas (Fig. 8 Ad). While at 6 months after the surgery, only the edges of the new bone tissue were fuchsia (Fig. 8 Ah). The percentages of PAS-stained signals at 3 and 6 months after the surgery in the material group were approximately equal to those in the normal group. In the MSC group, the percentage of PAS-stained signals was slightly and significantly higher than those in the other groups at 3 months ($P < 0.05$) and 6 months ($P < 0.01$) after the surgery, respectively (Fig. 8B1 & B2). These results show that combining the bone collagen matrix combined with hUC-MSCs can promote chondrocyte growth better than only the bone collagen matrix.

Effect of combining bone collagen matrix with hUC-MSCs on BMP-2 expression

The BMP-2 expression in tissues was detected by immunochemistry. At both 3 and 6 months after the surgery, only a small amount of BMP-2 was expressed at the osteocytes in the normal group (Fig. 9 Aa & Ae). Because the control group did not show any obvious bone repair, BMP-2 expression was not observed at either 3 or 6 months after the surgery (Fig. 9 Ab & Af). In the material group, the BMP-2 was mainly concentrated in the osteocytes and osteoclasts at the edge of the trabecular bone (Fig. 9 Ac & Ag). In the MSCs group, the BMP-2 was mainly expressed at the edge of the trabecular bone at 3 months after the surgery (Fig. 9 Ad), and in the area of new bone tissue growth at 6 months after the surgery (Fig. 9 Ah). The percentages of positive signals of BMP-2 at 3 and 6 months in the material and normal groups were approximately equal. In the MSC group, the percentage of BMP-2 positive signals was slightly and

significantly higher than those in the other groups at 3 months ($P < 0.05$) and 6 months ($P < 0.01$) after the surgery (Fig. 9B1 & B2). The results show that the ability of the bone collagen matrix combined with the hUC-MSCs to induce BMP-2 generation was better than that of the bone collagen matrix alone.

Proliferation And Apoptosis Analysis Of Bone Defect Site

TUNEL assays were used to detect apoptosis in the bone defect center of each group, and the apoptotic nuclei were stained brown (Fig. 10A). Ki67 immunohistochemistry was used to detect the proliferation of cells in the bone defect center of each group, and the proliferation cells were labeled with fluorescent green (Fig. 10B). Because no bone tissue had formed in the bone defect center of the control and material groups, the cell proliferation rate and apoptosis rate were statistically 0. The TUNEL results showed that the apoptosis rate in the MSCs group was significantly higher at 3 months after the surgery ($P < 0.05$) and lower at 6 months after the surgery ($P < 0.01$) than those in the normal group (Fig. 10C1). The Ki67 immunohistochemical results showed that the proliferation rate in MSCs group have an increasing trend at 3 months after the surgery and a decreasing trend at 6 months after the surgery as compared with normal groups, but there was no statistical difference (Fig. 10C2). Moreover, because the proliferating cells in the MSCs group were mainly concentrated in the bone growth area (Fig. 10Bh1), combining the bone collagen matrix with the hUC-MSCs effectively promote bone regeneration and repair by regulating cell proliferation and apoptosis.

Assessment Of Postoperative Health Status Of Rabbits

Blood routine (Table 1& Table 4), liver function (Table 2 & Table 5) and renal function (Table 3 & Table 6) were used to estimate the health status of the rabbits at 3 and 6 months after the surgery, and the data obtained for the normal and control groups were compared. The blood routine results showed that the lymphocyte (LYM) and neutrophil granulocyte (NEUT) concentrations decreased and increased, respectively, in the MSCs group at 3 months after the surgery, and both returned to normal at 6 months after the surgery. The C-reactive protein (CRP) concentration in the MSCs group was lower than that in the material and controls groups at both 3 and 6 months after the surgery. CRP concentration in the control group was higher than that in the normal group at 3 months and approximately equal to that in the normal group at 6 months after the surgery. These results suggest that the MSCs group has no obvious inflammatory response, and the control and MSCs groups both have exhibited an elevated inflammatory response at 3 months after the surgery, which returned to normal at 6 months after the surgery. The liver function results showed mildly abnormal aspartate aminotransferase (AST) and alanine aminotransferase (ALT) concentrations in the material group at 3 months after the surgery and normal concentrations at 6 months after the surgery, suggesting that the control group exhibited a mildly elevated inflammatory response at 3 months after the surgery, which returned to be normal at 6 months after the surgery. The ALP concentrations in the control, material and MSCs groups were higher and lower than those in the normal group at 3 and 6 months after the surgery, respectively, suggesting that the

concentration of osteoblasts had increased substantially at 3 months after the surgery and had normalised at 6 months after the surgery. Renal function results showed that the creatinine (CR) concentration was higher in the control and material groups, and that the blood urea nitrogen (BUN) and CR concentration were higher in the MSCs group at 3 months after the surgery. All the indicators were normal at 6 months after the surgery. To summarise, compared with the normal group, the control, material, and MSCs group all exhibited mild inflammatory responses at 3 months after the surgery. At 6 months after the surgery, all the indicators in each group had normalised. Moreover, the CRP concentration in the material group was higher than that in the MSC one at 6 months after the surgery, suggesting that adding the hUC-MSCs reduced the inflammatory response.

Table 1
Blood routine test results 3 months after surgery.

Detection index	Unit	Normal group	Control group	Material group	MSCs group
RBC	10^{12}/L	5.460 ± 0.128	5.460 ± 0.831	5.823 ± 0.888	4.423 ± 0.839
HCT	%	35.400 ± 0.852	36.933 ± 3.260	36.500 ± 5.335	26.767 ± 6.956
RDW-CV	10^9/L	13.000 ± 0.883	12.400 ± 1.122	14.133 ± 1.893	13.767 ± 1.517
RDW-SD	%	29.567 ± 2.089	29.933 ± 2.590	31.300 ± 2.780	34.267 ± 3.430
MCV	fL	64.833 ± 0.125	68.300 ± 4.607	62.867 ± 3.967	68.800 ± 1.042
HBG	g/L	116.333 ± 5.249	120.000 ± 13.736	117.333 ± 15.413	98.333 ± 20.072
MCH	pg	21.233 ± 0.492	22.100 ± 0.883	20.300 ± 1.499	22.267 ± 0.759
MCHC	g/L	327.667 ± 7.760	324.333 ± 9.031	322.333 ± 6.018	323.667 ± 11.728
WBC	10^9/L	12.417 ± 3.685	8.655 ± 0.845	9.860 ± 1.520	7.150 ± 0.260
LYM#	10^9/L	4.438 ± 0.978	2.682 ± 0.664	2.449 ± 1.107	2.286 ± 0.702
LYM%	%	36.663 ± 3.101	37.443 ± 1.827	35.227 ± 3.915	23.440 ± 2.310**##
NEUT#	10^9/L	5.462 ± 1.451	4.993 ± 0.642	5.598 ± 0.738	4.654 ± 0.096
NEUT%	%	55.833 ± 4.129	54.537 ± 4.425	55.047 ± 2.917	66.140 ± 1.662*#
MONO#	10^9/L	0.655 ± 0.145	0.335 ± 0.027	0.694 ± 0.183	0.533 ± 0.104
MONO %	%	5.463 ± 0.902	4.997 ± 1.387	6.340 ± 1.085	7.840 ± 1.146
EO#	10^9/L	0.209 ± 0.047	0.161 ± 0.034	0.260 ± 0.193	0.246 ± 0.151
EO %	%	1.747 ± 0.289	2.563 ± 1.269	3.210 ± 1.010	2.237 ± 0.439
BASO	10^9/L	0.033 ± 0.008	0.033 ± 0.018	0.013 ± 0.008	0.028 ± 0.009
BASO %	%	0.293 ± 0.103	0.460 ± 0.123	0.177 ± 0.076	0.343 ± 0.174

Mean SD values were calculated for each group. * represents the statistical difference between each group and the normal group. # represents the statistical difference between each group and the control group.*, # P0.05; **, ## P0.01.RBCred blood cell; HCT: hematocrit; RDW-CV: red blood cell volume distribution width; RDW-SD: red blood cell distribution width ; MCV: mean corpuscular volume ; HBG: hemoglobin; MCH: mean corpuscular hemoglobin; MCHC: mean corpuscular hemoglobin concentration; WBC: white blood cell;LYM: lymphocyte ;NEUT: neutrophile granulocyte; MONO: monocyte; EO: eosinophil; BASO: basophil; PLT: platelet; PDW: platelet distribution width; MPV: mean platelet volume; PLCR: platelet-large cell ratio; PCT: procalcitonin; CRP: C reactive protein.

Detection index	Unit	Normal group	Control group	Material group	MSCs group
PLT	10^9/L	155.333 ± 35.113	152.000 ± 17.682	123.333 ± 7.587	158.333 ± 32.602
PDW	%	16.100 ± 0.294	16.333 ± 0.419	15.633 ± 0.450	16.433 ± 0.660
MPV	fL	7.500 ± 0.283	7.600 ± 0.638	6.967 ± 0.262	7.200 ± 0.141
PLCR	%	17.000 ± 3.001	16.333 ± 2.530	11.600 ± 0.779	16.000 ± 3.024
PCT	%	0.043 ± 0.021	0.037 ± 0.005	0.018 ± 0.002	0.025 ± 0.011
CRP	mg/L	6.567 ± 1.195	11.75 ± 8. 380	16.465 ± 1.565	3.850 ± 0.650

Mean SD values were calculated for each group. * represents the statistical difference between each group and the normal group. # represents the statistical difference between each group and the control group.*, # *P*0.05; **, ## *P*0.01.RBCred blood cell; HCT: hematocrit; RDW-CV: red blood cell volume distribution width; RDW-SD: red blood cell distribution width ; MCV: mean corpuscular volume ; HBG: hemoglobin; MCH: mean corpuscular hemoglobin; MCHC: mean corpuscular hemoglobin concentration; WBC: white blood cell;LYM: lymphocyte ;NEUT: neutrophile granulocyte; MONO: monocyte; EO: eosinophil; BASO: basophil; PLT: platelet; PDW: platelet distribution width; MPV: mean platelet volume; PLCR: platelet-large cell ratio; PCT: procalcitonin; CRP: C reactive protein.

Table 2
Liver function test results in blood at 3 months postoperatively.

Detection index	Unit	Normal group	Control group	Material group	MSCs group
ALT	IU/L	45.267 ± 5.016	39.400 ± 10.500	73.267 ± 21.770	35.350 ± 0.650
AST	IU/L	30.500 ± 6.309	17.200 ± 0.100	43.567 ± 11.912	25.050 ± 3.250
ALP	IU/L	38.600 ± 2.900	45.433 ± 6.585	66.567 ± 14.946	56.000 ± 27.050
TP	g/L	53.533 ± 0.903	54.733 ± 2.522	54.367 ± 5.672	56.767 ± 2.549
ALB	g/L	31.633 ± 2.216	34.700 ± 2.471	34.833 ± 5.226	35.467 ± 0.309
GLB	g/L	21.867 ± 3.081	20.067 ± 1.967	19.500 ± 0.698	21.300 ± 2.273
A/G		1.487 ± 0.282	1.753 ± 0.257	1.783 ± 0.237	1.680 ± 0.159
TBIL	Umol/L	9.363 ± 1.095	7.280 ± 1.417	6.370 ± 1.410	11.030 ± 1.015#
DBIL	Umol/L	5.460 ± 0.235#	3.380 ± 0.511*	3.523 ± 0.288*	5.533 ± 0.903#
IBIL	Umol/L	4.650 ± 0.170	5.260 ± 0.050	3.785 ± 0.085*##	5.497 ± 0.284*

Mean SD values were calculated for each group. * represents the statistical difference between each group and the normal group. # represents the statistical difference between each group and the control group.*, # P 0.05; **, ## P 0.01. ALT:alanine aminotransferase; AST: aspartate aminotransferase; ALP: alkaline phosphatase; TP: total protein; ALB: albumin; GLB: globulin; TBIL: total bilirubin; DBIL: bilirubin direct; IBIL: indirect bilirubin.

Table 3
Renal function results test in blood at 3 months postoperatively.

Detection index	Unit	Normal group	Control group	Material group	MSCs group
BUN	**mmol/L**	7.277 ± 1.950	8.193 ± 1.576	9.697 ± 1.101	12.323 ± 2.768
CR	**mmol/L**	65.210 ± 6.462	102.250 ± 16.693	95.040 ± 3.693	88.985 ± 5.195
UA	**mmol/L**	31.467 ± 2.155	29.700 ± 0.000	29.800 ± 1.675	29.700 ± 0.000

Mean SD values were calculated for each group. * represents the statistical difference between each group and the normal group. # represents the statistical difference between each group and the control group.*, # P 0.05; **, ## P 0.01. BUN: blood urea nitrogen CR: creatinine UA: uric acid.

Table 4
Blood routine test results at 6 months postoperatively.

Detection index	Unit	Normal group	Control group	Material group	MSCs group
RBC	10^{12}/L	5.343 ± 0.191	5.443 ± 0.443	5.583 ± 0.961	5.040 ± 0.184
HCT	%	35.567 ± 1.281	38.467 ± 2.131	37.567 ± 5.236	32.633 ± 1.312
RDW-CV	10^9/L	12.800 ± 0.455	12.733 ± 0.403	13.167 ± 0.450	13.167 ± 0.094
RDW-SD	%	30.367 ± 2.660	32.233 ± 0.939	31.733 ± 1.247	30.567 ± 0.450
MCV	fL	66.667 ± 3.206	70.900 ± 2.670	67.700 ± 3.395	64.833 ± 0.544
HBG	g/L	122.000 ± 1.633	126.000 ± 7.483	122.667 ± 14.727	112.000 ± 2.160
MCH	pg	22.833 ± 0.694	23.033 ± 0.531	22.233 ± 1.576	22.267 ± 0.613
MCHC	g/L	343.000 ± 8.602	327.000 ± 11.045	327.333 ± 7.542	343.667 ± 9.741
WBC	10^9/L	12.057 ± 2.159	9.420 ± 0.243	15.217 ± 4.687	9.050 ± 1.040
LYM#	10^9/L	4.317 ± 0.868	3.157 ± 0.377	4.079 ± 0.942	2.920 ± 0.057
LYM%	%	35.680 ± 0.724	33.453 ± 3.371	27.387 ± 2.349*	32.600 ± 3.167
NEUT#	10^9/L	6.865 ± 1.266	5.553 ± 0.137	7.462 ± 0.064	5.380 ± 0.910
NEUT%	%	56.893 ± 0.696	58.997 ± 2.200	64.077 ± 2.309*	59.083 ± 3.129
MONO#	10^9/L	0.559 ± 0.023	0.507 ± 0.069	0.699 ± 0.072	0.460 ± 0.029
MONO %	%	4.777 ± 0.793	5.400 ± 0.861	5.973 ± 0.385	5.090 ± 0.332
EO#	10^9/L	0.290 ± 0.092	0.167 ± 0.039	0.305 ± 0.092	0.280 ± 0.071
EO %	%	2.443 ± 0.860	1.773 ± 0.424	2.023 ± 0.347	3.020 ± 0.399
BASO	10^9/L	0.025 ± 0.007	0.035 ± 0.002	0.078 ± 0.010**##	0.020 ± 0.008
BASO %	%	0.207 ± 0.066	0.377 ± 0.025	0.540 ± 0.086**	0.207 ± 0.090

Mean SD values were calculated for each group. * represents the statistical difference between each group and the normal group. # represents the statistical difference between each group and the control group.*, # P0.05; **, ## P0.01. RBCredblood cell; HCT: hematocrit; RDW-CV: red blood cell volume distribution width; RDW-SD: red blood cell distribution width; MCV: mean corpuscular volume; HBG: hemoglobin; MCH: mean corpuscular hemoglobin; MCHC: mean corpuscular hemoglobin concentration; WBC: white blood cell;LYM: lymphocyte;NEUT: neutrophile granulocyte; MONO: monocyte; EO: eosinophil; BASO: basophil; PLT: platelet; PDW: platelet distribution width; MPV: mean platelet volume; PLCR: platelet-large cell ratio; PCT: platelet volume; CRP: C reactive protein.

Detection index	Unit	Normal group	Control group	Material group	MSCs group
PLT	10^9/L	142.000 ± 18.184	142.000 ± 12.083	165.333 ± 36.335	148.000 ± 13.441
PDW	%	15.767 ± 0.125	16.300 ± 0.424	16.000 ± 0.294	16.200 ± 0.163
MPV	fL	7.000 ± 0.216	7.167 ± 0.262	6.967 ± 0.125	6.933 ± 0.386
PLCR	%	12.700 ± 0.648	15.000 ± 1.651	14.200 ± 1.633	14.600 ± 3.395
PCT	%	0.027 ± 0.012	0.030 ± 0.008	0.050 ± 0.024	0.027 ± 0.009
CRP	mg/L	3.863 ± 1.707	2.960 ± 0.536	9.920 ± 1.598	3.367 ± 0.838

Mean SD values were calculated for each group. * represents the statistical difference between each group and the normal group. # represents the statistical difference between each group and the control group.*, # *P*0.05; **, ## *P*0.01. RBCredblood cell; HCT: hematocrit; RDW-CV: red blood cell volume distribution width; RDW-SD: red blood cell distribution width; MCV: mean corpuscular volume; HBG: hemoglobin; MCH: mean corpuscular hemoglobin; MCHC: mean corpuscular hemoglobin concentration; WBC: white blood cell;LYM: lymphocyte;NEUT: neutrophile granulocyte; MONO: monocyte; EO: eosinophil; BASO: basophil; PLT: platelet; PDW: platelet distribution width; MPV: mean platelet volume; PLCR: platelet-large cell ratio; PCT: platelet volume; CRP: C reactive protein.

Table 5
Liver function test results in blood at 6 months postoperatively.

Detection index	Unit	Normal group	Control group	Material group	MSCs group
ALT	IU/L	61.533 ± 17.310	52.133 ± 15.964	37.300 ± 5.679	55.200 ± 9.335
AST	IU/L	22.400 ± 1.657	17.000 ± 1.800	21.000 ± 4.537	28.150 ± 0.650#
ALP	IU/L	67.433 ± 2.007#	44.300 ± 3.226*	38.800 ± 9.200*	44.150 ± 6.450*
TP	g/L	60.000 ± 3.289	59.133 ± 1.434	58.633 ± 7.013	57.133 ± 1.537
ALB	g/L	38.700 ± 1.424	39.633 ± 0.826	34.133 ± 7.643	38.100 ± 0.589
GLB	g/L	21.267 ± 1.837	19.500 ± 0.927	24.533 ± 3.991	19.033 ± 0.967
A/G		1.827 ± 0.096	2.043 ± 0.094	1.457 ± 0.520	2.007 ± 0.069
TBIL	Umol/L	5.027 ± 0.659	5.073 ± 1.377	5.573 ± 1.311	4.647 ± 0.898
DBIL	Umol/L	2.350 ± 0.530	3.093 ± 0.972	2.813 ± 0.821	2.913 ± 0.652
IBIL	Umol/L	2.677 ± 0.885	1.980 ± 0.743	2.325 ± 0.405	1.990 ± 0.140

Mean SD values were calculated for each group. * represents the statistical difference between each group and the normal group. # represents the statistical difference between each group and the control group.*, # P0.05; **, ## P0.01. ALT:alanine aminotransferase; AST: aspartate aminotransferase; ALP: alkaline phosphatase; TP: total protein; ALB: albumin; GLB: globulin; TBIL: total bilirubin; DBIL: bilirubin direct; IBIL: indirect bilirubin.

Table 6
Renal function results test in blood at 6 months postoperatively.

Detection index	Unit	Normal group	Control group	Material group	MSCs group
BUN	mmol/L	8.453 ± 0.097	7.730 ± 1.744	7.970 ± 1.032	9.510 ± 0.328
CR	mmol/L	90.983 ± 5.695	108.427 ± 11.757	96.057 ± 21.218	107.480 ± 5.195
UA	mmol/L	30.967 ± 0.694	29.467 ± 0.205	30.467 ± 0.818	29.700 ± 1.023

Mean SD values were calculated for each group. * represents the statistical difference between each group and the normal group. # represents the statistical difference between each group and the control group.*, # P0.05; **, ## P0.01. BUN: blood urea nitrogen; CR: creatinine; UA: uric acid.

Discussion

Bone induction refers to the induction of connective tissue adjacent to the bone graft area by bone growth factors or seed cells in the bone material. The formation of new bone is facilitated by affecting undifferentiated bone progenitor cells, promoting their differentiation and proliferation and eventually becoming osteoblast. Recently, MSCs have been used to induce bone regeneration in bone defect of orofacial clefts [23–25]. Human dental pulp stem cells are used to repair maxillary alveolar defects in rats [23]. Bone-marrow-derived mesenchymal stem/stromal cells (BM-MSCs) loaded in hydroxyl apatite/collagen promote local osteogenesis in alveolar cleft in rat and human [24, 25]. Although hUC-MSCs have also been used treat various diseases [26, 27], there are few reports about the use of hUC-MSCs in the treatment of alveolar process cleft.

HUC-MSCs are characterized by easy extraction, multidirectional differentiation, short proliferation time, low immunogenicity, and long survival time after transplantation and have, therefore, become the preferred seed cells for transplantation [28, 29]. In addition, because hUC-MSCs are obtained from neonatal umbilical cords. Neonatal umbilical cords are medical waste and no harm to the donor. And few ethical implications arise from using hUC-MSCs [30]. Moreover, the hUC-MSC stem cells obtained from umbilical cords show rapid self-renewal [31]. HUC-MSCs also express low levels of major histocompatibility complex II and costimulatory molecules, thereby reducing the possibility of rejection [32]. Other MSCs, such as BM-MSCs, have obvious osteogenic ability and low immunogenicity. However, their sources are limited. Furthermore, it is difficult to obtain such cells and easy to harm donors when the cells are collected [33, 34]. Therefore, compared with other MSCs, hUC-MSCs have more extensive application prospects.

The bone collagen matrix used in this study was a bone matrix prepared from de-greased and de-cellularised bovine cancellous bone. The decalcified and de-proteinised heterogeneous bone matrix was mainly composed of type 1 collagen, which is insoluble and highly hinged and exhibits good bone-guiding activity, toughness and strength. This material preserves the natural structure of the bone and exhibits the right-sized pores wherein cells and blood vessels can grow. Owing to the removal of antigens, the antigenicity of the material is very weak, and there were no obvious signs of rejection after implantation. Because the heterogeneous bone matrix is more widely derived than allogeneic bone, and can be bio-degraded and absorbed in a shorter time, it meets the requirements of the ideal carrier.

Studies have shown that the collagen biomaterials alone exhibited no obvious effective function in bone repair [35]. However, combining collagen bio-materials with a bone collagen matrix can slow the degradation of hUC-MSCs, thereby prolonging the bone repair time. Using collagen scaffold alone to repair rabbit alveolar cleft had no significant effect. Collagen scaffold material combined with hUC-MSCs can significantly repair rabbit alveolar cleft, and the defective jaw can be repaired to be close to the normal jaw. Our results are similar with Korn et al's study that hydroxyl apatite/collagen with MSCs can promote local osteogenesis in an animal model of alveolar cleft [24]. However, our work is different from Korn et al's study. Firstly, the sources of stem cells are different. MSCs used in our study were isolated from human umbilical cord. MSCs mentioned in Korn et al's study were isolated from rat bone marrow. Secondly, model animals are different. we used young female Japanese white rabbits. Korn et al's study

used adult rats. Thirdly, the modeling methods are different. In our study, the alveolar process cleft model was established by removing part of the jawbone equal to the volume of (1 cm · 0.5 cm · 0.4 cm) with a rongeur. In Korn et al's study, a localized bone defect with 3.3 mm in diameter was created using a diamond-coated cylindrical shaped drill in the mid-palatal suture. Our model lacked bone on three sides and was difficult to induce bone regeneration. Therefore, it is more likely to be useful to evaluate the bone regeneration capacity of biomaterials.

In order to evaluate the quality of the newly formed bone in the defect area, the bone trabeculae and mineral density in the centre of the cubic bone-defect area were detect by Micro CT analysis. Although bone collagen matrix alone did not significantly increase the bone defect area, it induced partial bone regeneration. The percentage of bone trabeculae and bone density is visibly higher in MSCs group than material group, but significantly less than normal bone. These facts showed that combining bone collagen matrix with hUC-MSCs could enhance the quality of the newly formed bone in the defect area, but it doesn't reach the normal level.

The repair of bone defect generally involves in osteogenesis, the collagen distribution and chondrogenesis [36]. Here, combining bone collagen matrix with hUC-MSCs contributed to the repair of the bone defect in the alveolar process cleft, likely through promoting the expression of osteoblasts, chondrocytes, type 1 collagen and BMP-2. Our experimental results also showed that the apoptosis rate of the MSCs group was significantly higher than that of the normal group at 3 months after surgery and significantly lower than that of the normal group at 3 months after surgery. The trend was similar with cell proliferation. Usually, apoptosis is a ubiquitous phenomenon for the natural, developmental cell death and takes place in proliferating cell populations and is involved in tissue morphogenesis [37–39]. Therefore, we speculated that the increase of apoptosis in MSCs group at 3 months after surgery was due to the increase of proliferative cells. At 6 months, the cell proliferation level was downward and the corresponding apoptosis rate was decreased.

The results of the blood analysis suggested that combining bone collagen matrix with hUC-MSCs could inhibit the inflammatory response. There was report showed that hUC-MSCs may play a role in bone tissue repair by inhibiting inflammation [21]. Therefore, we speculate that combining bone collagen matrix with hUC-MSCs promotes new bone formation in the alveolar process cleft possibly through restraining inflammatory response.

Recent studies have shown that MSCs exhibit a short survival time and poor cell differentiation activity in animal models [40, 41]. Furthermore, the conditioned media (CM) of MSCs can also induce inflammatory repair and tissue re-generation [41–43]. Therefore, it is believed that implanted MSCs repair tissues mainly by changing the local micro-environment rather than directly transforming into target cells because the cells involved in tissue repair are mainly cells of the receptor itself, which are homed by the paracrine regulation of MSCs and further proliferate and differentiate [40].

Conclusions

In the rabbit alveolar process cleft model, combining bone collagen matrix with hUC-MSCs could repaired the damaged bone tissue and promoted the new bone regeneration via improving osteogenesis, the collagen distribution and chondrogenesis. The study shows that the combining of hUC-MSCs with a bone collagen matrix is a promising strategy for building and repairing bone tissue in regenerative medicine.

Abbreviation

Japanese white rabbits (JWRs)
Human umbilical cord mesenchymal stem cells (hUC-MSCs)
Micro focus computerized tomography (micro CT)
Hematoxylin eosin (HE)
Alkaline phosphatase (ALP)
Periodic Acid-Schiff stain (PAS)
Immunohistochemical (IHC)
TdT-mediated dUTP nick-end Labelling (TUNEL)
Bone gla protein (BGP)

Declarations

Acknowledgements

The authors are very grateful to the National Key Research and Development Program of China We are also very grateful to the animal experiment center of the National Research Institute for Family Planning for its meticulous care of animals.

Funding

This work was funded by grants from the National Key Research and Development Program of China (2016YFC1000803).

Availability of data and materials

All data generated or analyzed during this study are included in this published article.

Authors’ contributions

XCS, XM and HFX designed the study. XCS, HW and JHL were responsible for the vivo surgery and performing the procedure. YFY and LQY provided the bone repair materials. HW and DZ were responsible for in vitro experiments. XCS, HW and HFX prepared the manuscript. XCS, HW, DZ and HFX were responsible for revising the manuscript critically for important intellectual content. All authors read and approved the final manuscript.

Ethical Approval

Ethical approval to report this case was obtained from the National Research Institute for Family Planning (Ethics Number 2015-16).

Consent for publication

All authors gave consent for publication.

Competing interests

The authors declare that they have no competing interests.

Statement of Informed Consent

There are no human subjects in this article and informed consent is not applicable.

Statement of Human and Animal Rights

All procedures in this study were conducted in accordance with the National Research Institute for Family Planning (Ethics Number 2015-16) approved protocols.

Code availability

Not applicable.

References

1. Cohen M, Figueroa AA, Haviv Y, Schafer ME, Aduss H. Iliac versus cranial bone for secondary grafting of residual alveolar clefts. *Plast Reconstr Surg*; 1991, 87(3):423–427.
2. Tai CC, Sutherland IS, McFadden L. Prospective analysis of secondary alveolar bone grafting using computed tomography. *J Oral Maxillofac Surg*. 2000; 58(11):1241–1249.
3. LaRossa D, Buchman S, Rothkopf DM, Mayro R, Randall P. A comparison of iliac and cranial bone in secondary grafting of alveolar clefts. *Plast Reconstr Surg*. 1995; 96(4):789–797; discussion 798–799.
4. Rosenthal RK, Folkman J, Glowacki J, Demineralized bone implants for nonunion fracture, bone cysts, and fibous lesins. *Clin Orthop Relat Res*. 1999; (364): 61–69.
5. Al-Asfour A, Farzad P, Andersson L, Joseph B, Dahlin C. Host tissue reactions of non-demineralized autogenic and xenogenic dentin blocks implanted in a non-osteogenic environment. An experimental study in rabbits. *Dent Traumatol*. 2014; 30(3):198–203
6. Smith BT, Santoro M, Grosfeld EC, Shah SR, van den Beucken JJJP, Jansen JA, Mikos AG. corporation of fast dissolving glucose porogens into an injectable calcium phosphate cement for bone tissue engineering. *Acta Biomater*. 2017; 50: 68–77.
7. Liu S, Hou KD, Yuan M, Peng J, Zhang L, Sui X, Zhao B, Xu W, Wang A, Lu S, Guo Q. Characteristics of mesenchymal stem cells derived from Wharton's jelly of human umbilical cord and for fabrication of non-scaffold tissue-engineered cartilage. *J Biosci Bioeng*. 2014; 117(2): 229–235.

8. Tassi SA, Sergio NZ, Misawa MYO, Villar CC. Efficacy of stem cells on periodontal regeneration: Systematic review of pre-clinical studies. *J Periodontal Res*. 2017; 52(5): 793–812.
9. Jin YZ, Lee JH. Mesenchymal stem cell therapy for bone regeneration. *Clin Orthop Surg*. 2018; 10(3): 271–278.
10. Hämmerle CH, Chiantella GC, Karring T, Lang NP. The effect of a deproteinized bovine bone mineral on bone regeneration around titanium dental implants. *Clin Oral Implants Res*. 1998; 9(3):151–162.
11. Tatić Z, Stamatović N, Bubalo M, Jancić S, Racić A, Miković N, Tatić N, Rakić M. Histopathological evaluation of bone regeneration using human resorbable demineralized membrane. *Vojnosanit Pregl*. 2010; 67(6):480–486.
12. Lee JS, Wikesjö UM, Jung UW, Choi SH, Pippig S, Siedler M, Kim CK. Periodontal wound healing/ regeneration following implantation of recombinant human growth/ differentiation factor-5 in a beta-tricalcium phosphate carrier into one-wall intrabony defects in dogs. *J Clin Periodontol*. 2010; 37(4):382–389.
13. Ruehe B, Niehues S, Heberer S, Nelson K. Miniature pigs as an animal model for implant research: bone regeneration in critical-size defects. *Oral Surg Oral Med Oral Pathol Oral Radiol Endod*. 2009; 108(5):699–706.
14. Liu Y, Zheng Y, Ding G, Fang D, Zhang C, Bartold PM, Gronthos S, Shi S, Wang S. Periodontal ligament stem cell-mediated treatment for periodontitis in miniature swine. *Stem Cells*. 2008; 26(4):1065–1073.
15. Schmitz JP, Hollinger JO. The critical size defect as an experimental model for craniomandibulofacial nonunions. *Clin Orthop Relat Res*. 1986; (205): 299–308.
16. Gallego L, Junquera L, García E, García V, Alvarez-Viejo M, Costilla S, Fresno MF, Meana A. Repair of rat mandibular bone defects by alveolar osteoblasts in a novel plasma-derived albumin scaffold. *Tissue Eng Part A*. 2010; 16(4):1179–1187.
17. Puumanen K, Kellomäki M, Ritsilä V, Böhling T, Törmälä P, Waris T, Ashammakhi N. A novel bioabsorbable composite membrane of Polyactive 70/30 and bioactive glass number 13–93 in repair of experimental maxillary alveolar cleft defects. *J Biomed Mater Res B Appl Biomater*. 2005; 75(1):25–33.
18. Kamal M, Andersson L, Tolba R, Bartella A, Gremse F, Hölzle F, Kessler P, Lethaus B. A rabbit model for experimental alveolar cleft grafting. *J Transl Med*. 2017;15(1): 50.
19. Djasim UM, Hekking-Weijma JM, Wolvius EB, van Neck JW, van der Wal KG. Rabbits as a model for research into craniofacial distraction osteogenesis. *Br J Oral Maxillofac Surg*. 2008; 46(8): 620–624.
20. Sun XC, Zhang ZB, Wang H, Li JH, Ma X, Xia HF. Comparison of three surgical models of bone tissue defects in cleft palate in rabbits. *Int J Pediatr Otorhinolaryngol*. 2019; 124: 164–172.
21. Zhang L, Li Y, Guan CY, Tian S, Lv XD, Li JH, Ma X, Xia HF. Therapeutic effect of human umbilical cord-derived mesenchymal stem cells on injured rat endometrium during its chronic phase. *Stem Cell Res Ther*. 2018; 9(1): 36.

22. Dominici M, Le Blanc K, Mueller I, Slaper-Cortenbach I, Marini F, Krause D, Deans R, Keating A, Prockop Dj, Horwitz E. Minimal criteria for defining multipotent mesenchymal stromal cells. *The International Society for Cellular Therapy position statement. Cytotherapy*. 2006;8(4):315–317.
23. Jahanbin A, Rashed R, Alamdari DH, Koohestanian N, Ezzati A, Kazemian M, Saghafi S, Raisolsadat MA. Success of maxillary alveolar defect repair in rats using osteoblast-differentiated human deciduous dental pulp stem cells. *J Oral Maxillofac Surg*. 2016; 74(4): 829.e1-9.
24. Korn P, Hauptstock M, Range U, Kunert-Keil C, Pradel W, Lauer G, Schulz MC. Application of tissue-engineered bone grafts for alveolar cleft osteoplasty in a rodent model. *Clin Oral Investig*. 2017; 21(8): 2521–2534.
25. Gimbel M, Ashley RK, Sisodia M, Gabbay JS, Wasson KL, Heller J, Wilson L, Kawamoto HK, Bradley JP. Repair of alveolar cleft defects: reduced morbidity with bone marrow stem cells in a resorbable matrix. *J Craniofacial Surg*. 2007;18(4):895–901.
26. Xu Y, Meng H, Li C, Hao M, Wang Y, Yu Z, Li Q, Han J, Zhai Q, Qiu L. Umbilical cord-derived mesenchymal stem cells isolated by a novel explantation technique can differentiate into functional endothelial cells and promote revascularization. *Stem Cells Dev*. 2010; 19(10): 1511–1522.
27. Wang N, Xiao Z, Zhao Y, Wang B, Li X, Li J, Dai J. Collagen scaffold combined with human umbilical cord-derived mesenchymal stem cells promote functional recovery after scar resection in rats with chronic spinal cord injury. *J Tissue Eng Regen Med*. 2018; 12(2): e1154-e1163.
28. Cao FJ, Feng SQ. Human umbilical cord mesenchymal stem cells and the treatment of spinal cord injury. *Chin Med J (Engl)*. 2009;122(2): 225–231.
29. Baksh D, Yao R, Tuan RS. Comparison of proliferative and multilineage differentiation potential of human mesenchymal stem cells derived from umbilical cord and bone marrow. *Stem Cells*. 2007; 25(6): 1384–1392.
30. Wang L, Tran I, Seshareddy K, Weiss ML, Detamore MS. A comparison of human bone marrow-derived mesenchymal stem cells and human umbilical cord-derived mesenchymal stromal cells for cartilage tissue engineering. *Tissue Eng Part A*. 2009; 15(8): 2259–2266.
31. Ding DC, Chang YH, Shyu WC, Lin SZ. Human umbilical cord mesenchymal stem cells: a new era for stem cell therapy. *Cell Transplant*. 2015; 24(3): 339–347.
32. De Miguel MP, Fuentes-Julián S, Blázquez-Martínez A, Pascual CY, Aller MA, Arias J, Arnalich-Montiel F. Immunosuppressive properties of mesenchymal stem cells: advances and applications. *Curr Mol Med*. 2012; 12(5): 574–591.
33. Takushima A, Kitano Y, Harii K. Osteogenic potential of cultured periosteal cells in a distracted bone gap in rabbits. *J Surg Res*. 1998; 78(1): 68–77.
34. Barry FP, Murphy JM. Mesenchymal stem cells: clinical applications and biological characterization. *Int J Biochem Cell Biol*. 2004; 36(4): 568–584.
35. Hollinger JO, Schmitt JM, Buck DC, Shannon R, Joh SP, Zegzula HD, Wozney J. Recombinant human bone morphogenetic protein-2 and collagen for bone regeneration. *J Biomed Mater Res*. 1998; 43(4): 356–364.

36. Gurtner GC, Werner S, Barrandon Y, Longaker MT. Wound repair and regeneration. *Nature*. 2008; 453 (7193): 314–321.
37. Tilly JL, Tilly KI, Perez GI. The genes of cell death and cellular susceptibility to apoptosis in the ovary: a hypothesis. *Cell Death Differ*. 1997; 4(3):180–187.
38. Takamoto N, Leppert PC, Yu SY. Cell death and proliferation and its relation to collagen degradation in uterine involution of rat. *Connect Tissue Res*. 1998;37(3–4):163–175.
39. Pellicciari C, Bottone MG, Schaack V, Barni S, Manfredi AA. Spontaneous apoptosis of thymocytes is uncoupled with progression through the cell cycle. *Exp Cell Res*. 1996; 229(2): 370–377.
40. Kotobuki N, Katsube Y, Katou Y, Tadokoro M, Hirose M, Ohgushi H. In vivo survival and osteogenic differentiation of allogeneic rat bone marrow mesenchymal stem cells (MSCs). *Cell Transplant*. 2008; 17(6): 705–712.
41. An JH, Park H, Song JA, Ki KH, Yang JY, Choi HJ, Cho SW, Kim SW, Kim SY, Yoo JJ, Baek WY, Kim JE, Choi SJ, Oh W, Shin CS. Transplantation of human umbilical cord blood-derived mesenchymal stem cells or their conditioned medium prevents bone loss in ovariectomized nude mice. *Tissue Eng Part A*. 2013; 19(5–6): 685–696.
42. Kinnaird T, Stabile E, Burnett MS, Shou M, Lee CW, Barr S, Fuchs S, Epstein SE. Local delivery of marrow-derived stromal cells augments collateral perfusion through paracrine mechanisms. *Circulation*. 2004; 109(12): 1543–1549.
43. Linero I, Chaparro O. Paracrine effect of mesenchymal stem cells derived from human adipose tissue in bone regeneration. *PLoS One*. 2014; 9(9): e107001.

Figures

Figure 1

A activated collagen matrix ; B the collagen membrane; C surgical process: a normal rabbit b The collagen membrane was trimmed and the bone collagen matrix was inoculated with hUC-MSCs. c the rabbit after anesthesia. d open the oral cavity after anesthesia. e-f remove the maxillary bone of equal volume. g measure the size of the bone that has been removed. h add materials i add collagen membrane. j suture the skin.

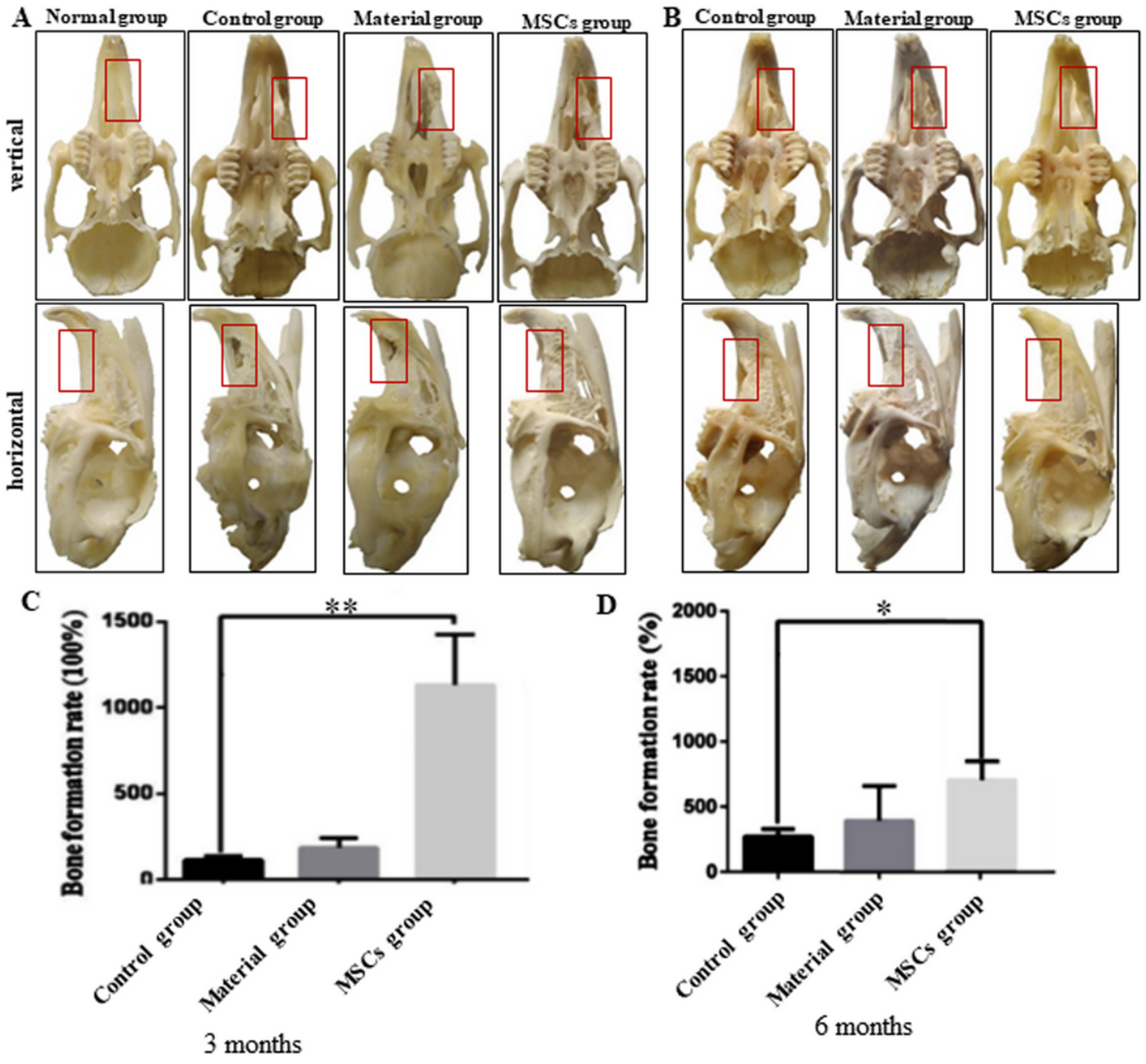

Figure 2

The general appearance of the skull. A the general appearance of the skull 3 months after surgery; B the general appearance of the skull 6 months after surgery. The red box shows the postoperative appearance

of the transplanted area. The rabbits were randomly assigned to four groups: normal group, control group, material group and MSCs group. The normal group was fed normally. In the control group, only collagen membrane covered bone defect site. In material group, bone collagen matrix was implanted bone defect site and collagen membrane covered the injury site. In MSCs group, combining bone collagen matrix with hUC-MSCs was implanted bone defect site and collagen membrane covered the injury site. C and D The bone formation rate at 3 months and 6 months after the surgery, respectively. * P<0.05, **P<0.01.

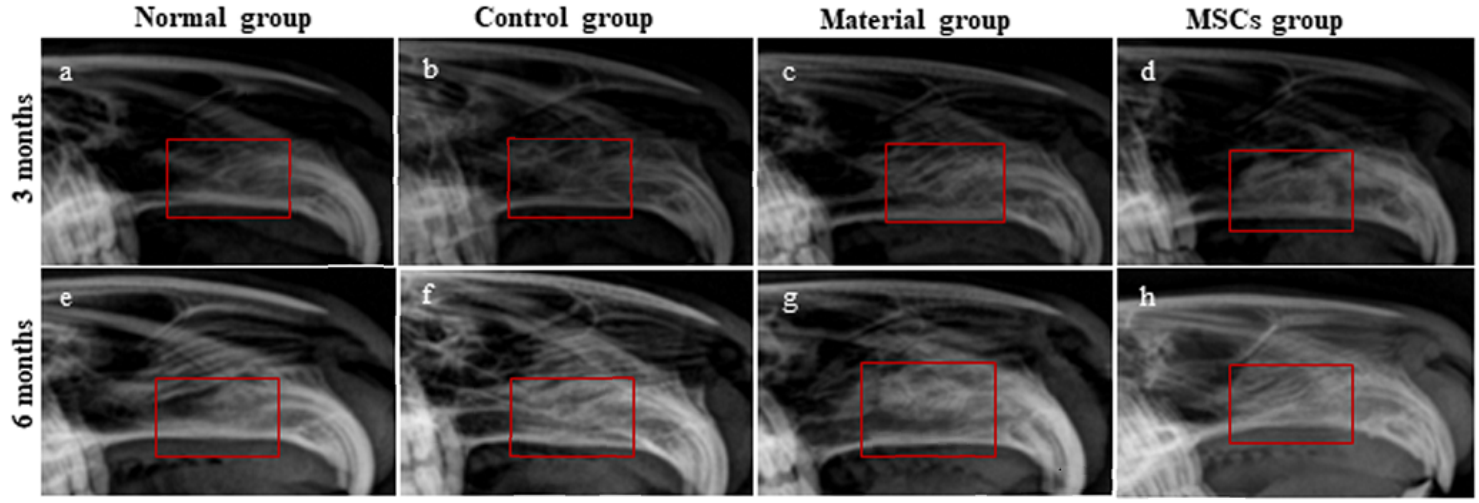

Figure 3

X-ray analysis results. a-d X-ray analysis of the skull 3 months after surgery; e-h X-ray analysis of the skull 6 months after surgery. a, e Normal group; b, f Control group; c, g Material group; d, h MSCs group. The red box is the surgical area. After the rabbits were under mild anesthesia, the left maxilla was scanned.

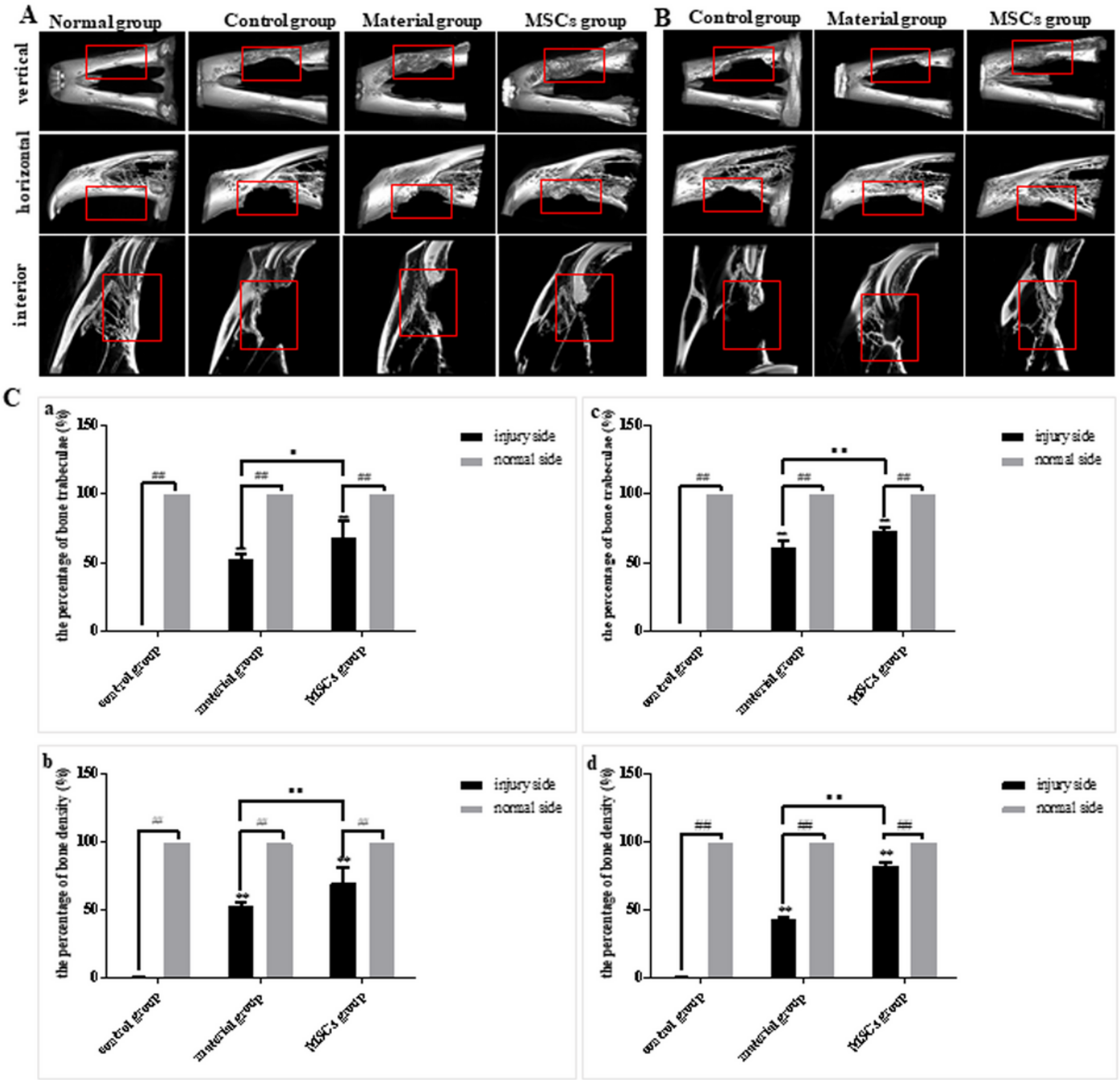

Figure 4

Micro CT results. A CT images from different angles 3 months after surgery; B CT images from different angles 6 months after surgery; C-a The percentage of bone trabeculae 3 months after surgery; C-b The percentage of bone density 3 months after surgery; C-c The percentage of bone trabeculae 6 months after; C-d The percentage of bone density 6 months after surgery. The injury side of each group was compared with that of the control group and the difference was denoted by *. The difference between the injury side and the normal side was expressed as #. The difference between the material group and the MSCs group on the injury side was expressed by *. *P□0.05, **P□0.01, ##P□0.01, ##P□0.01. The arrow indicated the surgical area. The surgical area of the skull model was placed in the scanning area of the

Mirco CT for scanning. Two - and three - dimensional image processing and bone mineral density data acquisition were performed on the scanning results. Finally, the bone mineral density data were statistically analyzed.

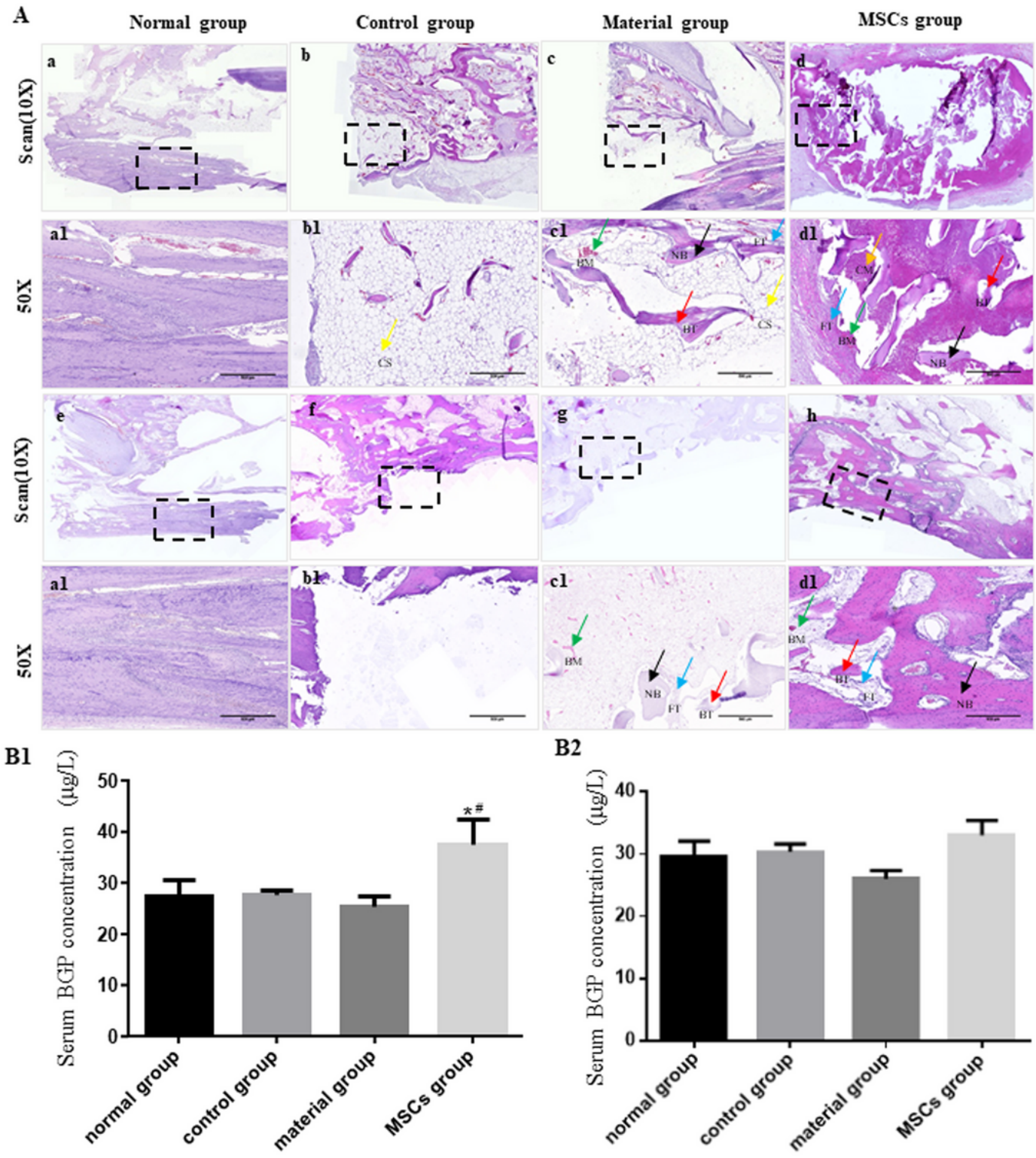

Figure 5

A HE staining results. a, e & a1, e1 Normal group; b, f & b1, f1: Control group; c, g & c1, g1: Material group; d, h& d1, h1: MSCs group. a-h The scan results of HE staining. a1-h1 The result of HE staining after 50

times magnification. BM: bone marrow (green arrow); FT: fibrous tissue (blue arrow); BT: bone trabecular (red arrow); CM: collagen materials (orange arrow); NB: new bone (black arrow); CS: cavitation structure (yellow arrow). B1 Serum BGP levels 3 months after surgery; B2 Serum BGP levels 6 months after surgery. The injury side of each group was compared with that of the control group and the difference was denoted by *. The difference between the injury side and the normal side was expressed as #. #P□0.05 , *P□0.05.

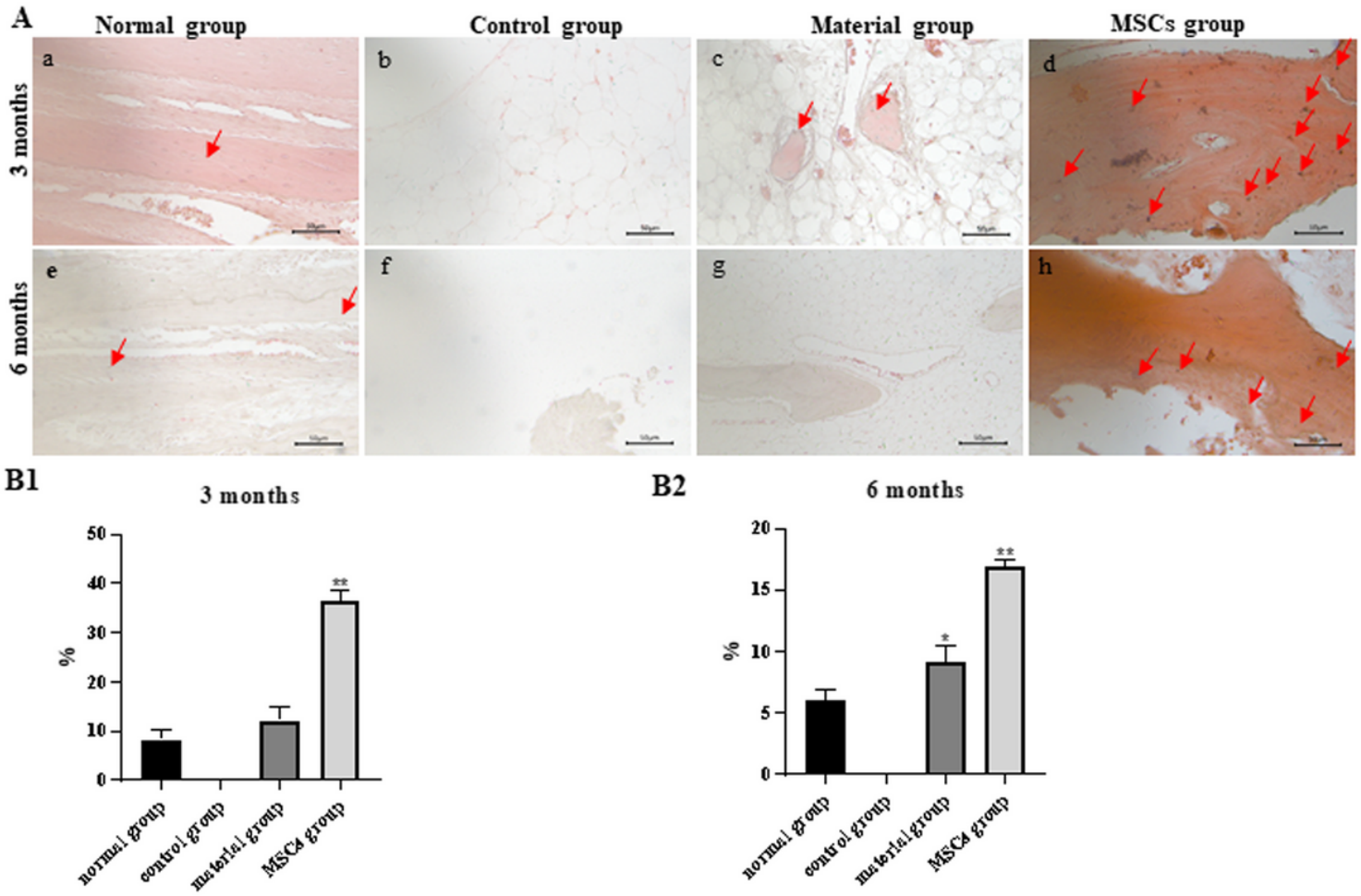

Figure 6

ALP staining results (200×). A: a-d ALP staining results 3 months after surgery; e-h ALP staining results 6 months after surgery. a, e Normal group; b, f Control group; c, g Material group; d, h MSCs group. Mark the area of the positive signal with a red arrow. B1: Percentage of cells expressing ALP at 3 months after surgery. B2: Percentage of cells expressing ALP at 6 months after surgery. * Represents the statistical difference between each group and the normal group. * P < 0.05; ** P < 0.01.

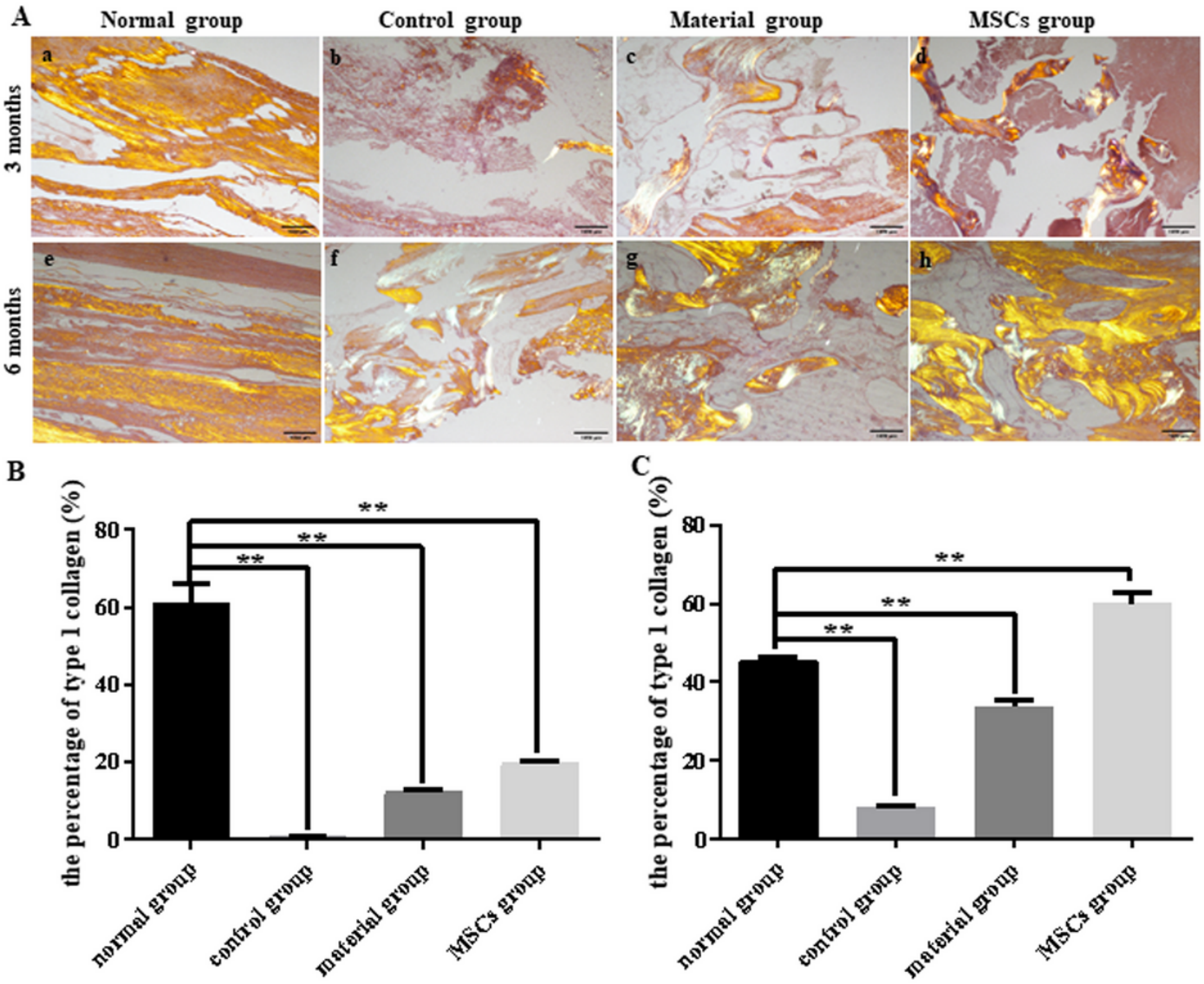

Figure 7

Sirius red staining results (40×). A a-d Sirius red staining results 3 months after surgery; e-h Sirius red staining results 6 months after surgery. a, e Normal group; b, f Control group; c, g Material group; d, h MSCs group. Mark the area of the positive signal with a red arrow. B The percentage of type 1 collagen 3 months after surgery. C The percentage of type 1 collagen 6 months after surgery. All groups were compared with the Normal group, and the statistical difference was denoted by *. ** P□0.01. Type I collagen stained with Sirius red appears bright orange under polarized light microscopy.

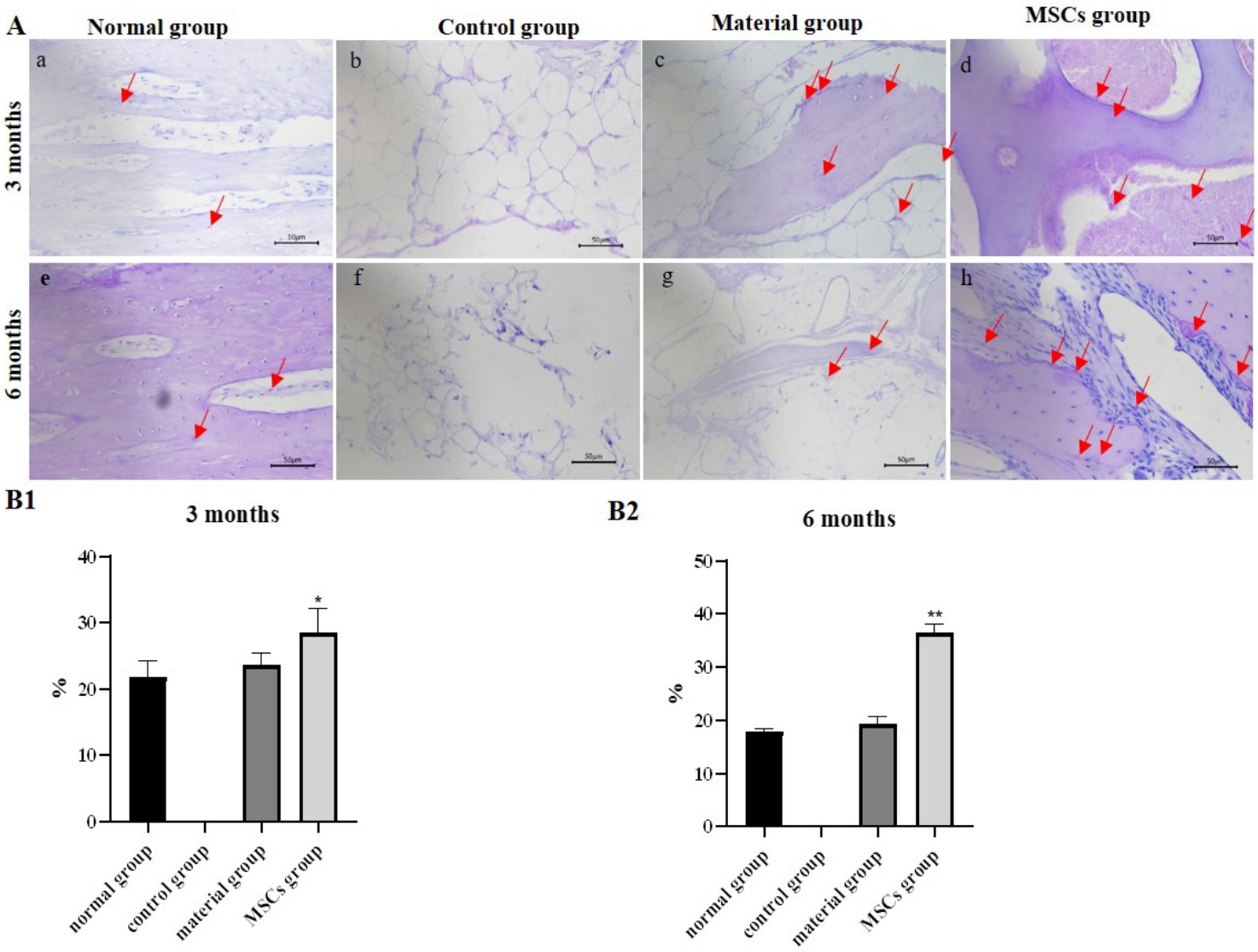

Figure 8

PAS staining results (200×). A: a-d PAS staining results 3 months after surgery; e-h PAS staining results 6 months after surgery. a, e Normal group; b, f Control group; c, g Material group; d, h MSCs group. Mark the area of the positive signal with a red arrow. B1: Percentage of cells expressing PAS at 3 months after surgery. B2: Percentage of cells expressing PAS at 6 months after surgery. * Represents the statistical difference between each group and the normal group. * $P < 0.05$; ** $P < 0.001$.

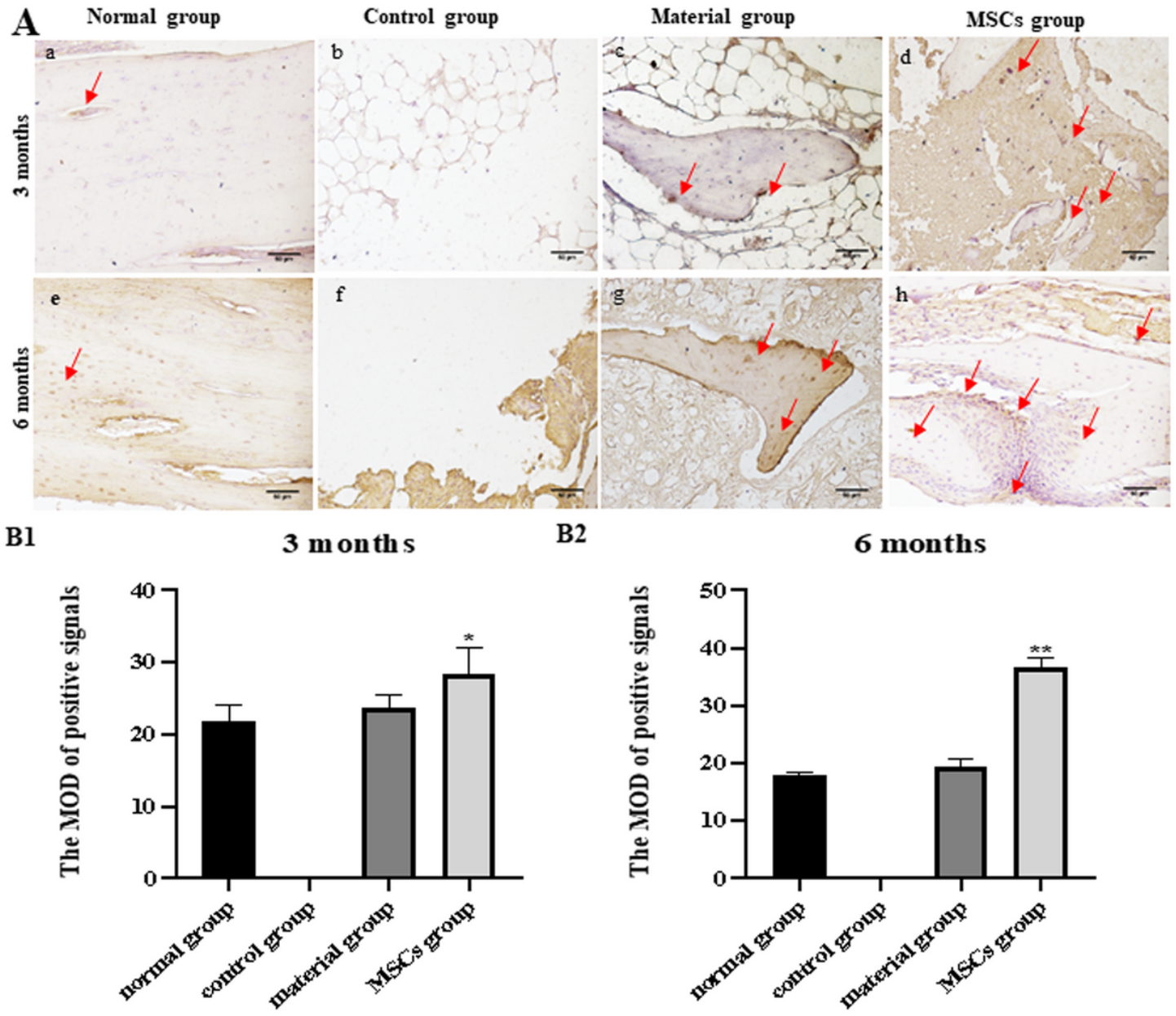

Figure 9

IHC results of BMP-2 (200×). A: a-d IHC results of BMP-2 3 months after surgery; e-h IHC results of BMP-2 6 months after surgery. a, e Normal group; b, f Control group; c, g Material group; d, h MSCs group. Mark the area of the positive signal with a red arrow. B1: The MOD of positive signals at 3 months after surgery. B2: The MOD of positive signals at 6 months after surgery. * Represents the statistical difference between each group and the normal group. * $P < 0.05$; ** $P < 0.01$.

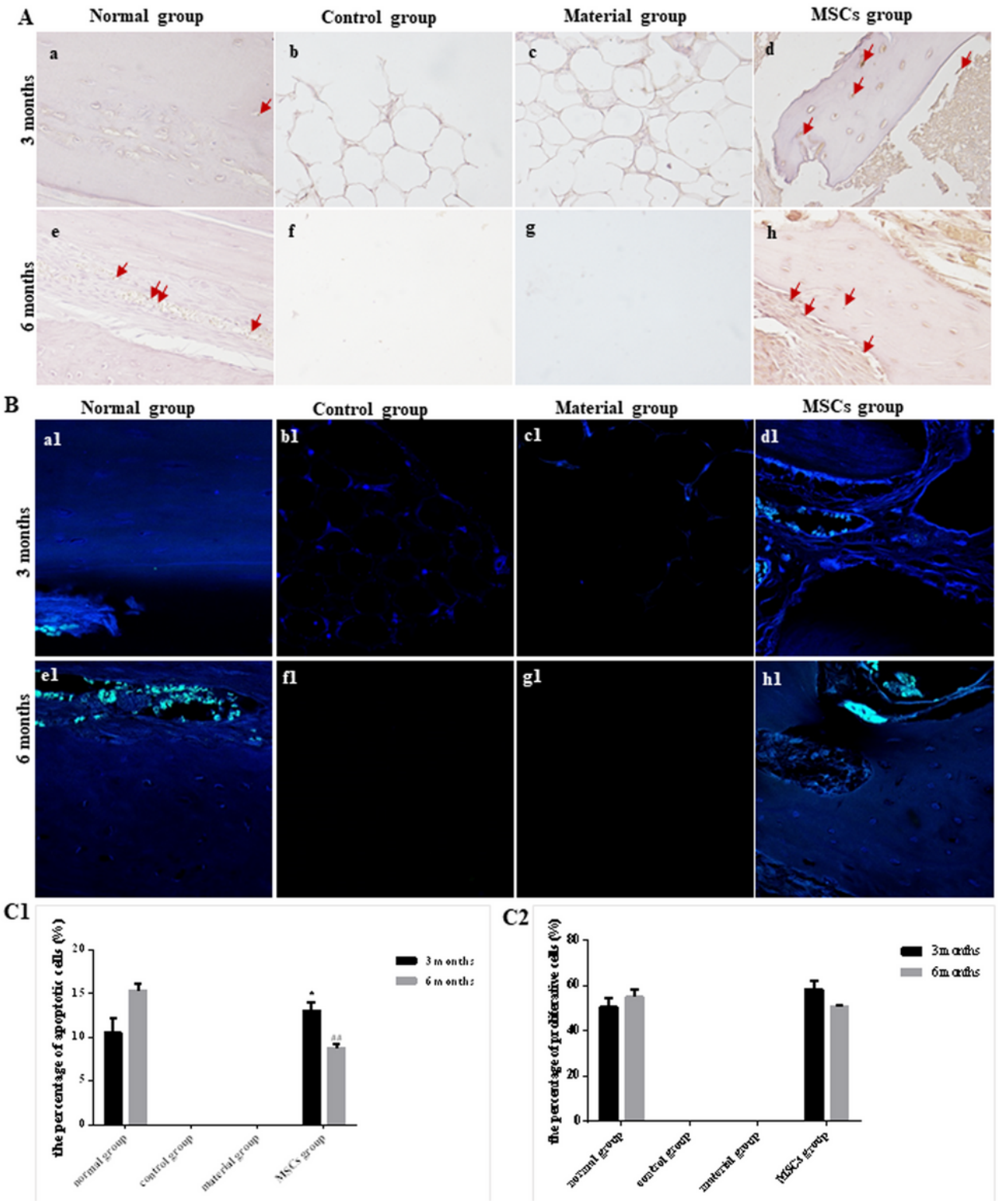

Figure 10

A TUNEL results (400×). B Ki67 results (400×). a-d & a1-d1 Results 3 months after surgery; e-h&e1-h1 Results 6 months after surgery. a, e & a1, e1 Normal group; b, f & b1, f1 Control group; c, g&c1,g1 Material group; d, h&d1,h1 MSCs group. C1 The percentage of apoptotic cells in each group at 3 or 6 months. C2 The percentage of proliferative cells in each group at 3 or 6 months. Cells labeled in green represent cells

that are proliferating. * Represents the statistical difference between each group and the normal group. # represents the statistical difference between each group and the normal group. *P < 0.05; # # P < 0.01.

Supplementary Files

This is a list of supplementary files associated with this preprint. Click to download.

- GraphicalAbstract.jpg